Available online at www.sciencedirect.com
ScienceDirect
Earth and Planetary Science Letters 265 (2008) 466–474
EPSL
www.elsevier.com/locate/epsl

Why meter-wide dikes at oceanic spreading centers?

Ran Qin *, W. Roger Buck

Lamont-Doherty Earth Observatory of Columbia University, United States

Received 11 October 2006; received in revised form 13 October 2007; accepted 17 October 2007
Available online 1 November 2007
Editor: C.P. Jaupart

Abstract

Numerical models show that maximum dike width at oceanic spreading centers should scale with axial lithospheric thickness if the pre-diking horizontal stress is close to the Andersonian normal faulting stress and the stress is fully released in one dike intrusion. Dikes at slow-spreading ridges could be over 5 m wide and maximum dike width should decrease with increasing plate spreading rate. However, data from ophiolites and tectonic windows into recently active spreading ridges show that mean dike width ranges from 0.5 m to 1.5 m, and does not clearly correlate with plate spreading rate. Dike width is reduced if either the pre-diking horizontal stress difference is lower than the faulting stress or the stress is not fully released by a dike. Partial stress release during a dike intrusion is the more plausible explanation, and is also consistent with the fact that dikes intrude in episodes at Iceland and Afar. Partial stress release can result from limited magma supply when a crustal magma chamber acts as a closed source during dike intrusions. Limited magma supply sets the upper limit on the width of dikes, and multiple dike intrusions in an episode may be required to fully release the axial lithospheric tectonic stress. The observation of dikes that are wider than a few meters (such as the recent event in Afar) indicates that large tectonic stress and large magma supply sometimes exist.

Keywords: dike; width; mid-ocean ridges; magma supply; dike episode; magma chamber

1. Introduction

Dikes are planar cracks filled with magma. In oceanic spreading centers, either back-arc spreading centers or mid-ocean ridges, basaltic dikes intrude repeatedly and form most of the oceanic crust (Delaney et al., 1998; Einarsson and Brandsdottir, 1980; Fialko and Rubin, 1998; Kidd, 1977; Sohn et al., 1998). Dike intrusions release magma and volatiles into the ocean, perturbing hydrothermal vents and triggering a sequence of related physical, chemical, and biological processes (Delaney et al., 1998). Given the central role of dike intrusions in plate spreading and related biological processes, sheeted dikes in ophiolites representing ancient oceanic crust have been extensively studied (Kidd, 1977). In recent years technological improvements also have made real-time monitoring and on-site experiments to study dike intrusions at active oceanic spreading centers possible.

The planar geometry of a dike makes the dike width as an easy-to-measure parameter that permits the most direct comparison between theoretical predictions and field observations. For example, dike width is directly tied to the frequency of dike events in a ridge of given spreading rate, which is essential for us to plan on-site experiments

* Corresponding author. LDEO 305 Oceanography, 61 RT. 9W, Palisades, NY10964, United States.
E-mail address: rqin@ldeo.columbia.edu (R. Qin).

0012-821X/$ - see front matter © 2007 Elsevier B.V. All rights reserved.
doi:10.1016/j.epsl.2007.10.044

at spreading ridges. Dike width is also thought to be a key factor controlling dike thermal cooling rate, dike propagation distance and speed and the persistence of fissure eruptions (Bruce and Huppert, 1989; Fialko and Rubin, 1998; Lister, 1995). These factors are essential to the understanding of ridge segmentation and magma transportation and distribution along ridge axis.

As we will detail below, basaltic dikes are nearly meter-wide, on average, across all oceanic spreading centers where field data are available. Though various processes may affect the width of a basaltic dike (Valentine and Krogh, 2006), it is generally accepted that basaltic dikes at oceanic spreading centers open as a result of elastic expansion of host rock under magma overpressure (Fialko and Rubin, 1998; Lister, 1995; Pollard et al., 1983). Since oceanic spreading centers have different thermal and mechanical structures (Purdy et al., 1992), it is important to know why the dike widths across different tectonic settings have the same average. However, previous studies calculating dike width by simply assuming 10–20 MPa uniform driving pressure failed to account for tectonic conditions, including the variations of driving pressure and dike height across different spreading centers (Fialko and Rubin, 1998; Pollard et al., 1983; Rubin, 1990; Rubin and Pollard, 1988).

Rather than treating a dike as a uniformly pressurized crack in an elastic half-space, in this study we compute possible stress distributions before and after dike intrusions in a way that accounts for a reasonable strength structure of the spreading center and the level of magma supply from magma chamber. Another advantage compared with previous studies is that we calculate the dike top and bottom using Weertman's method (Weertman, 1973) and do not assign the dike an arbitrarily determined dike height. We will show that limited magma supply controls the dike width.

2. Statistics of field data on dike width

Dike width measurements from active and fossil spreading centers (mid-ocean ridges and back-arc spreading centers) are readily available. In this study we use data from ophiolites from Oman (Umino et al., 2003), Troodos (Kidd, 1977), Betts Cove (Kidd, 1977) and Bay of Islands (Rosencrantz, 1983) in Newfoundland, Josephine of California (Harper, 1984), Ballantrae in Scotland (Oliver and McAlpine, 1998) and ancient dike swarms in Iceland (Gudmundsson, 1983; 1995); dike events monitored during Krafla 1975–1985 in Iceland (Tryggvason, 1994) and dikes exposed at Hess deep (unpublished data, J. Karson). Since September 2005, several dikes have intruded along the Dahabbu segment in Afar, East Africa (Wright et al., 2006).

Table 1 shows the number of dikes collected from these areas, inferred spreading rate, and the mean dike width. Since the dike width has either a power-law or log-normal distribution (Gudmundsson, 1983; 1995; Kidd, 1977; Rosencrantz, 1983), standard error is not a good description and we arbitrarily choose an upper band of dike width to help indicate dike width distribution, within which 80% of the dike measurements lies. The dike width is defined as the space between two chilled margins that indicates a single dike intrusion or 2 times the width if one chilled margin is missing (Kidd,

Table 1
Statistics of data on dike thickness

Spreading center	Inferred spreading rate[a]	Mean width (m)	Upper limit that contains 80% data (m)	Number of measurements
Hess Deep[b]	13 cm/yr, fast	0.56	0.64	37
Oman ophiolite (Umino et al., 2003)	Intermediate to fast	0.71	1.3	1511
Troodos ophiolite (Kidd, 1977)	Intermediate	1.58	2.4	530
Josephine ophiolite (Harper, 1984)	Intermediate to slow	~0.60	N/A	>600
Ballantrae ophiolite (Oliver and McAlpine, 1998)	N/A	0.50	1.03	137
Newfoundland ophiolite	Slow	0.48 (Kidd, 1977)	0.7	190
		0.80 (Rosencrantz, 1983)	1.2	576
Iceland	2.0 cm/yr, slow	0.8 (Tryggvason, 1994)	1.0	9
		~1.0[c] (Gudmundsson, 1995)	~2.0	>5000
Afar, East Africa Rift	1.0 cm/yr, slow	<5.0–6.0[d]	/	Several

[a] Fast means full spreading rate > 8 cm/yr, slow means < 4 cm/yr and intermediate falls between.
[b] Unpublished data from J. Karson.
[c] Tertiary dike swarms, A. Gudmundsson, pers. comm.
[d] Dike swarm recorded beginning September 2005.

1977). Treating the width of a single-side-chilled dike as one half of that of an intact dike increases the distribution spread, but the mean dike width will stay the same as long as both sides of the split dikes have the same possibility to be exposed in the field. In tectonic windows exposing upper oceanic crust in active submarine ridges, the chilled margin is hard to identify and laterally continuous, roughly parallel structural discontinuities are taken as dike margins [J. Karson, pers. comm.]. The published dike width data from Iceland ((Gudmundsson, 1983; 1995); A. Gudmundsson, per. comm.) only show the total width of dikes, most of which are composite dikes composed of several columnar cooling joints or multiple dikes that comprise many chilled margins. Since these dikes are thought to form by successive intrusions of multiple dikes, we will not use the published data directly (Gudmundsson, 1983; 1995). Instead, 0.5–2.0 m wide columnar joints formed as dikes cool and shrink and ~1.0 m estimations of mean dike width by Gudmundsson (1995) are listed in Table 1. There are also sparse data from Blanco Transform Zone of Juan de Fuca Ridge (Karson et al., 2002) and Kane Transform Zones of Mid-Atlantic Ridge (Karson, 1999) show that the dikes are commonly 0.5–1.5 m wide. Geodetic measurements made during the Krafla. Iceland dike intrusion episode of 1975–1984 show that most of these ~20 events involved opening of about a meter. The only significantly wider dike of that sequence was the first event. Another dike intrusion sequence in very slow-spreading environment is now occurring in Afar, Ethiopia, and the first dike in that sequence averaged 5–6 m wide, while later dikes have been narrower (Wright et al., 2006; Tim Wright, pers. comm. 2007). Although there is variability involved in dike width measurements, most dikes are contained in a small width range. In sum, dike width measurements in oceanic spreading centers show two important characteristics: (1) there is no clear relation between dike width and spreading rate; (2) the mean dike width is around 0.5–1.5 m.

3. Dike width from simple elastic calculation

3.1. Model setup

3.1.1. Simplified view of dike intrusion at oceanic spreading center

We consider a simplified 2-D ridge system with a lithosphere that is thinnest at the axis overlying hot, weak asthenosphere (Fig. 1). The oceanic plates move away from each other at the ridge axis and asthenosphere creeps to accommodate the deformation, stressing the lithosphere only. The thickness and geometry of

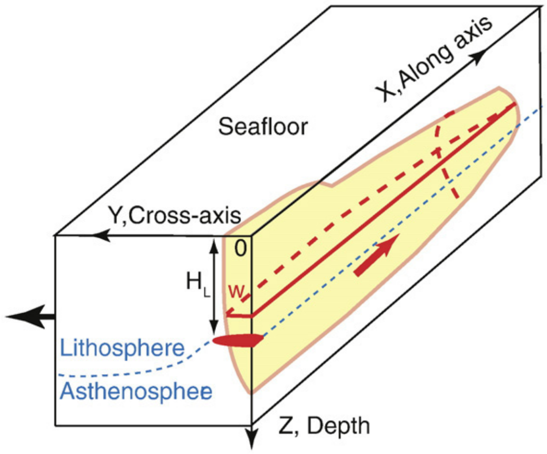

Fig. 1. Schematic view of dike intrusions at spreading centers. A typical ridge system has an axially-thinned lithosphere overlying hot asthenosphere. The plate is stretching constantly and in the long term the lithosphere is stressed but the hot, weak asthenosphere is relaxed. A dike originating from the crustal magma chamber at the bottom of the lithosphere may propagate both vertically and horizontally.

the lithosphere is controlled by thermal structure that varies at different plate spreading rates. Dikes originate from a magma chamber located at the bottom of the lithosphere and intrude vertically, following the direction of least horizontal stress coinciding with the direction of ridge axis. A dike could propagate both vertically upward to the surface and/or downward into the asthenosphere.

3.1.2. Rock density and mechanical properties

The rocks in oceanic spreading centers are layered, and their densities increase from the seafloor toward the mantle. For simplicity we assume the lithosphere has a uniform density ρ_l and the asthenosphere has density ρ_a. We choose diabase as the representative host rock bounding the dike wall and describe its mechanical property by visco-elastoplastic rheology. Viscous flow is considered Newtonian, and elastoplasticity is characterized by Mohr–Coulomb failure criteria. The Poisson's ratio of diabase has a small range between 0.22 and 0.28 and here we choose a mean $\nu=0.25$. The experimentally determined shear modulus for diabase is 27–42 GPa (Birch, 1966), however, the rock is much weaker at a larger scale where macro-cracks or faulting planes would largely control the rock behavior (Rubin, 1990). Seismic velocity data from Iceland (Foulger et al., 2003), the East Pacific Rise (Crawford and Webb, 2002) and the Mid-Atlantic Ridge (Barclay et al., 1998) show the S-velocity of upper crust (layer2, lava and sheeted dikes) gradually increases from 1.0 km/s to

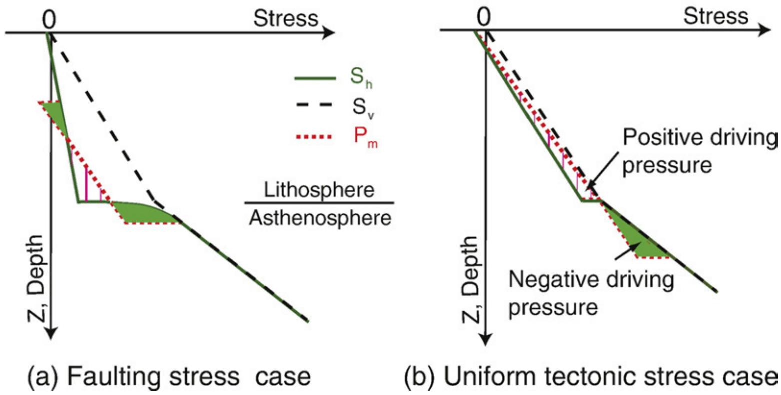

Fig. 2. Two examples of stress distributions at ridge axis. Dotted line shows the vertical stress S_v, solid curve is the horizontal stress S_h on the ridge axis before a dike intrusion and dashed line is the magma pressure P_m after dike intrusion. Driving pressure in a dike is the difference between P_m and S_h. (a) Andersonian normal faulting stress case, in which the ridge has been stretched to faulting and the resulting horizontal stress reaches a minimum. (b) Uniform tectonic stress case, in which the horizontal stress is uniformly lowered by S_d from lithostatic level. Note that the driving pressure is negative in the asthenosphere.

3.5 km/s, and P-velocity increases from 2.0 km/s to 6.0 km/s. Using a simple relation between seismic velocity and shear modulus, we could put shear modulus in the range of 3 GPa to 35 GPa. For illustrative purpose we only show one calculation with shear modulus G=10 GPa and 20 GPa (Fig. 4), and in the rest of the calculations only G=10 GPa is considered.

3.1.3. Stress in the dike

The horizontal stress at the ridge axis S_h (Fig. 2) is the stress acting on the dike wall prior to a dike intrusion. At oceanic spreading centers the horizontal stress is continuously lowered by plate spreading in the absence of fault slip or dike intrusions. We will detail later what might be a reasonable stress conditions at ridge axis, but here we simply present two simple views of the stress condition for comparison (Fig. 2): Andersonian normal faulting stress or a uniform stress tectonically lowered by S_d. Thus we can express the horizontal stress for $z \leq H_l$ (Turcotte and Schubert, 2002), in the normal faulting case:

$$S_h(z) = \rho_l g z - \frac{2\mu(\rho_l - \rho_w)gz + 2c}{\sqrt{\mu^2+1}+\mu}, \tag{1a}$$

or in the uniform stress case:

$$S_h(z) = \rho_l g z - S_d, \tag{1b}$$

For $z > H_l$ in both cases:

$$S_h(z) = \rho_l g H_l + \rho_a g(z - H_l) - (\rho_l g z - S_h)|_{z=H_l} \cdot e^{E/R\left(\frac{1}{T(z)} - \frac{1}{T_t}\right)} \tag{1c}$$

where z is the depth measured from the seafloor. The stress is assumed to be continuous at z=H_l. H_l is the thickness of axial lithosphere. $T(z)$ is the temperature linearly increasing with depth from T_t=273 K at the seafloor and T_t=873 K is the reference temperature at lithosphere–asthenosphere boundary. Cohesion is c=10.0 MPa, and friction coefficient μ=tan 30°. Activation energy E=276 kJ/mol, and gas constant R=8.31. As extensive fractures and fissures are seen at seafloor and may reach considerable depth, the horizontal stress $S_h(z)$ may not be lower than water pressure $\rho_w gz$ and in the model we put water pressure as the minimum to which the horizontal stress could drop. Water density is ρ_w=1000 kg/m^3.

Upon a sudden dike intrusion, the ridge axis is cracked open, and the magma is assumed to fill the dike up to the top. Given the low viscosity of hot magma and the time required to freeze that magma, we assume that the pressure in the intruding dike is equal to the static magma pressure, P_m. The magma pressure P_m in the dike at depth z=H_l, equals the pressure of magma chamber and decreases/increases towards the dike top/bottom at a constant gradient, $\rho_m g$. Therefore the pressure in the dike can be written as

$$P_m(z) = P_0 + \rho_m g(z - H_l) \tag{2}$$

where P_0 is the pressure in the magma chamber and the density of magma is ρ_m=2800 kg/m^3.

3.1.4. Dike top and bottom

If the driving pressure is high, the dike may reach the seafloor and feed fissure eruptions. However a dike penetrating downward may be hard to thermally arrest because the dike in the hot asthenosphere cools too slowly to freeze in a few days. A likely way to arrest downward dike propagation is a negative driving pressure in the asthenosphere, where the stress condition is close to lithostatic and the density of asthenosphere is higher than the magma. Fig. 2 shows how negative driving pressure, $P_m - S_h$, could be generated in the asthenosphere as the magma pressure gradient falls below the horizontal stress gradient. To determine the position of dike top and bottom, we use the method first given by Weertman (1973). This method traces the opening of a dike tip and regards the points where the dike tip changes from opening to closure as the position where dike propagation stops.

We use a 2-D boundary element program, TWODD (Crouch and Starfield, 1983), to calculate the elastic deformation of a dike in a non-gravitational half-space. Such a 2-D model can be justified as long as the extent of a dike along axis is several times larger than height of the dike. We try different positions of the top and bottom of the dike and use TWODD to see if they are sites of opening or closing bottom (Weertman, 1973). Comparing TWODD results with Weertman's analytical solution, the penetration depth calculated from both methods agrees within 1% when the number of elements is greater than ~50 (Qin et al., 2007).

3.2. Numerical results of dike width

Previous studies (Pollard et al., 1983) indicate that dike width, w, scales with rock properties (the shear modulus G, and Poisson's ratio v), mean driving pressure, $(P_m - S_h)$, and dike height, H, as:

$$w \propto \frac{(P_m - S_h)H}{G/(1-v)}. \tag{3}$$

Eq. (3) indicates that dike width increases with driving pressure and dike height but inversely depends on shear modulus. However, as we will discuss below, our numerical results suggest that Eq. (3) can only be used as a general guide since the lithospheric stress distribution and dike penetration depth also affect the dike width.

Fig. 3 shows how the dike opening changes along the dike wall, under different horizontal stress conditions: Andersonian normal faulting stress or uniform tectonic stress $S_d = 10$ MPa. In both cases the magma pressure is so high that the dike could propagate to the seafloor. Both the dike width and shape vary between two loading conditions. For the uniform tectonic stress case (Figs. 2(b) and 3 dashed line), the same magnitude of stress near the dike top will open the dike wider than if it does on the dike bottom. The resulting dike opening is like a triangle with the wide side near the top. In contrast, the faulting stress case has a more triangular stress distribution and the resulting dike opening is fairly uniform along most of the dike wall. Because dike width varies with depth, we pick the dike width in the middle of the lithosphere as the mean dike width, which may better compare with the field data, considering that the portion of the dike in the asthenosphere may be easily smeared by viscous creep flows or hard to expose at the surface.

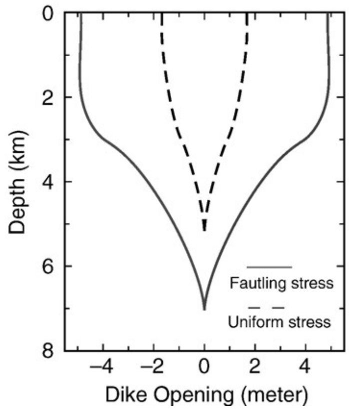

Fig. 3. The calculated dike opening varying with depth under both stress conditions. Dike opening in the faulting stress case is basically constant with depth until near the dike bottom, while in the uniform tectonic stress case dike opening progressively decreases from top to bottom. In the uniform tectonic stress case, because the stress distribution is uniform, the resulting dike opening is like a triangle. The faulting stress distribution is like a triangle, and the dike opening is more uniform with depth.

We plot mean dike width against axial lithosphere thickness in Fig. 4, along with the dike width data from ophiolites, Iceland, and Hess deep (see Table 1). Both stressing conditions are shown and in each case, two values of shear modulus are considered: 10 MPa and 20 MPa. Dike width deceases linearly with the shear modulus as predicted in Eq. (3). The dike width increases nearly with the square of axial lithosphere thickness in the faulting stress case, but only linearly with lithosphere thickness in the uniform tectonic stress case. In both cases the mean dike width is readily above the narrow 0.5–1.5 m range of field data when lithosphere thickness is greater than 1.0 km.

4. Reconciling the numerical results and field data: limited magma supply

The active and fossil spreading centers from which the dike width data are collected (Table 1) present a wide

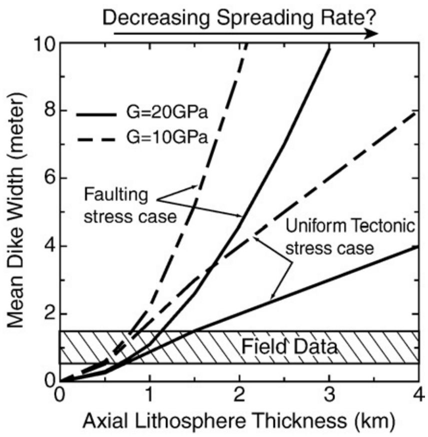

Fig. 4. Numerically modeled dike width increases with axial lithosphere thickness. The mean dike width is measured in the middle of the lithosphere. Hatched region indicates mean dike width from field observations (Table 1). Dashed curves have shear modulus G = 10 GPa and solid curves of 20 GPa. In faulting stress cases the dike width increases quadratically with lithosphere thickness, while in uniform stress case this trend is basically linear.

spectrum of spreading rates. Axial lithosphere thickness in oceanic spreading centers generally decreases with plate spreading rate, as inferred from seismic data and predicted by theoretical models (Purdy et al., 1992; Sinton and Detrick, 1992). Fast spreading ridges typically have an axial lithosphere thickness of 1–2 km, approximately the depth of the magma chamber (Sinton and Detrick, 1992). Axial lithosphere of intermediate spreading ridges may be 2–3 km thick, which is inferred from the presence of magma chamber on some ridge segments (Baran et al., 2005). No magma chamber reflectors have been imaged at slow-spreading ridges but 3–5 km deep seismic LVZ's (low-velocity zones) detected at the centers of some slow-spreading segments may indicate the sites of ephemeral magma bodies (Purdy et al., 1992).

Slow-spreading segment centers have thinner lithosphere than do segment ends where the lithosphere may be 3–7 km thick (Lin and Parmentier, 1989; Magde and Sparks, 1997). A very clearly imaged low-velocity zone at the center of the Krafla Segment in Iceland has a depth of 3 km (Brandsdottir et al., 1997). Iceland is a sub-aerial slow-spreading ridge where seismic and geodetic measurements show that dikes away from the segment center may reach 6–8 km depth (Gudmundsson, 1983; Rubin, 1990).

The model calculations in Fig. 4 show that (1) dikes in oceanic spreading centers can be over 2.0 m wide if the lithosphere is thicker than 1.0 km; and (2) maximum dike width increases with axial lithosphere thickness. Clearly the modeled dike widths are not consistent with the field data in terms of averages and the trend with spreading rate (Table 1, Fig. 4). This discrepancy between the modeled dike width and field data has to be explained by a reduction in driving pressure, $(P_m - S_h)$ during dike propagations, since other factors (e.g. the shear modulus, G, Poisson's ratio, ν) that should affect the dike width (see Eq. (3)) are reasonably constrained and are not likely to vary with spreading rate. The driving pressure, $(P_m - S_h)$, could be reduced either by increasing the pre-diking horizontal stress, S_h, above the level needed for extensional faulting or by decreasing the magma pressure, P_m, in the dike wall during the dike propagation.

It is possible that dikes are triggered well before pre-diking horizontal stress, S_h, reaches the minimum stress, i.e., Andersonian normal faulting stress level. For example, a basaltic dike may be triggered due to magma chamber overpressure built up by continuous magma flux (Kelemen and Aharonov, 1998). For this idea to work, the pre-diking horizontal stress has to be higher (closer to the lithostatic stress condition) for ridges with thicker lithosphere to not produce wider dikes. However, there is no reason to assume that the horizontal stress is higher for ridges with thicker lithosphere, as these ridges typically develop rift valleys and are extensively faulted.

There is strong evidence suggesting pre-diking stresses at ridges are very close to or at the faulting stress level. The world stress map shows that there are active normal faults from earthquake focal mechanism solutions all along the slow and intermediate spreading ridges (South Indian Ridge, Mid-Atlantic Ridge and Iceland, for example) (Reinecker et al., 2004). Fault scarps reach tens of meters high in Iceland and hundreds of meters at intermediate and slow-spreading ridges, where 1–2 km deep rifted valleys are also present at the ridge axis (Lin and Parmentier, 1989; Tryggvason, 1994). At fast spreading ridges it is not clear that the horizontal stress is also lowered to the level of Andersonian normal faulting, though extensive fissures (Wright et al., 1995) and fresh faulted surfaces (Macdonald et al., 1996) as well as increasing seismic activities before fissure eruptions (Tolstoy et al., 2006) indicate that this is a good possibility. The observations as well as the measured time interval between are consistent with the idea that dikes are triggered by earthquake activity close to magma chamber tops (Buck, 2006) and these earthquakes may only happen when stresses approach the yield stress.

Therefore, the only feasible explanation for the meter-wide dike may be that magma pressure in the magma chamber, P_0, is much lower than the maximum allowed, so that the magma pressure in the dike wall is lower

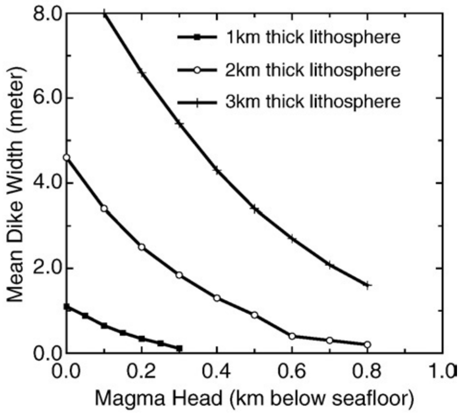

Fig. 5. Mean dike width decreases as the magma pressure in the dike drops. The magma pressure is indicated by magma head that is measured as the distance from the dike top to the seafloor. A meter-wide dike is produced when the magma head drops by an amount that depends on the lithosphere thickness.

(Eq. (2)). Pressure reduction in a crustal magma chamber during dike intrusions only happens when the magma supply is limited. By limited magma supply we mean that the magma chamber is closed system during the time span of dike propagation. The magma pressure drops as the dike takes magma out the magma chamber. Fig. 5 shows model results indicating how the dike width decreases as magma head drops. Here the magma head is defined as the level that fluid magma could reach, measured relative to the seafloor. Magma pressure is related to head by gravitational acceleration, g, times the density contrast between magma and water. The magma head is zero if the magma could reach the surface and is negative if the magma pressure is lower. A meter-wider dike could be produced if the magma pressure in the dike drops low enough.

Magma supply, however, does not explain why very narrow dikes are seldom observed. As a dike propagation pulls more magma from a source region the pressure and width of the dike should diminish. The rate at which magma flows in a propagating dike should decrease as the dike narrows and will eventually allow freezing of the magma. The width at which freezing occurs depends on several things including the country rock temperature and magma viscosity, but for 0.5–1 m is a width for freezing (Bruce and Huppert, 1989; Fialko and Rubin, 1998; Lister, 1995).

The idea that the magma pressure drops as a result of limited magma supply fits into the picture of a small and thin magma chamber seismically imaged within a broader mush zone (Sinton and Detrick, 1992). Assuming a Mogi source (Mogi, 1958), ~0.1% volume change of magma chamber produces 10–20 MPa of pressure loss if the shear modulus of oceanic crust is 10–20 GPa, a pressure change about a −500 m magma head loss (Fig. 5). This pressure change may cause the surface subsidence above the magma source. For example, geodetic measurements of Krafla 1975 intrusion/eruption episodes indicate that surface deflation above the caldera always accompanies fissure eruptions (Einarsson and Brandsdottir, 1980; Tryggvason, 1994).

Regional stress variations may explain why some dikes are much wider than a meter. In regions of fairly uniform stress a dike should propagate as long as it is wide enough that it does not freeze (Buck et al., 2006). As it propagates more magma is removed from the magma chamber, pressure there and in the dike is reduced and so the dike narrows until it freezes. Dikes that encounter stress barriers (where the relative tension is less) could stop and in some cases open to greater widths. This may explain the observation that the first dike in the 1975–1984 Krafla episode was at least 3 m wide (Tryggvason, 1994) and the September, 2005 dike of the ongoing Afar, Ethiopia episode was more than 5–8 m wide (Wright et al., 2006).

5. Implications of limited magma supply for dike episodes

Limited magma supply allows the possibility that single dike intrusions might not release all the stress

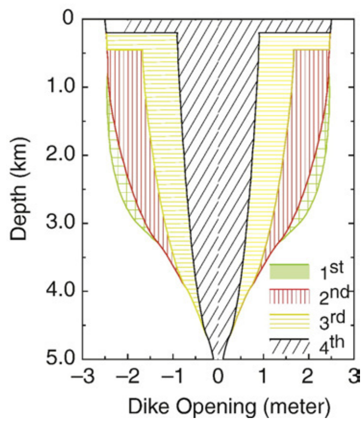

Fig. 6. Multiple meter-wider dikes could intrude in a diking episode due to limited magma supply as in this set of model calculations. The magma head at the end of each intrusion is −0.85 km, −0.40 km, −0.2 km and 0.0 km respectively. The lithosphere is 3.0 km thick, shear modulus G=30 GPa and the horizontal stress prior to the first intrusion is at faulting stress level. The first dike did not reach the seafloor; the following dikes opened fissures to the seafloor, but do not have enough magma to fill the opening, leaving a surface depression. Only the last dike feeds extrusives.

accumulated during an amagmatic spreading period. An episode of dikes is thus needed to fully release the stress to restore the ridge axis to a lithostatic state. Fig. 6 shows how successive meter-wide dike intrusions may relieve the stress in the axial lithosphere. The first dike does not reach the seafloor, and only releases part of the axial stress, though such a dike might generate extensive fissures or faulting at the seafloor. The second dike might reach the seafloor, but as the dike opens and propagates, the magma head falls below the seafloor. The third and fourth dike reaches the seafloor, feeds fissure eruptions and further releases the strain. More dikes may intrude later depending on magma availability. In such an episode each dike is meter-wide and the total width is several meters.

We thus expect one dike episode at a ridge segment would persist for the time needed to release accumulated stress, depending on the time for the magma chamber to replenish between dike intrusions. The ridge segment may then have no intrusions for tens of years at fast spreading ridges and hundreds of years at slow-spreading ridges to allow strain accumulation for the next episode. The longer quiescence time for slower spreading ridges corresponds to the longer time needed to accumulate higher tectonic stress because of the slower spreading rate and thicker lithosphere. The quiescence time between episodes may be also related to magma flux at the ridge axis, as available magma is another necessity to feed multiple dike intrusions (Kelemen and Aharonov, 1998). Submersible surveys on lava flows in mid-ocean ridges and observations of sub-aerial spreading centers like Iceland suggest a correlation between spreading rate and eruption frequency (Buck et al., 2006; Sinton et al., 2002). Episodic basaltic dike eruptions at certain continental settings are also linked to magma volume, where tectonic stretching is thought to be the controlling mechanism (Valentine and Perry, 2007).

A good example of a dike episode is the 1975 episode of Krafla rift zone in Iceland. That section of plate boundary remained quiet for about 250 yr, but beginning in 1975 more than ten meter-wide dikes intruded within 10 yr and created 7.0–9.0 m opening at Krafla rift zone (Tryggvason, 1994). The distance and direction of dike propagation varied systematically in a way that reflects the gradual release of tectonic stresses in an episode (Buck et al., 2006). The Krafla rift zone has been basically inactive since 1984, and this episodic intrusion/eruption style contrasts sharply with Kilauea volcano of Hawaii that had continuous eruptions for over 100 yr and is still active today (Macdonald et al., 1986). Both areas are hot-spot influenced, but their different eruption styles may suggest that Krafla rift zone is tectonic stress guided while Kilauea is magma surge controlled.

6. Summary

If the horizontal stress prior to a dike intrusion is close to the extensional faulting stress and magma pressure is sufficient to allow magma to reach the surface during an intrusion, our numerical results demonstrate that modeled dike width: (1) is over 3 times larger than the observed average and; (2) should scale with axial lithosphere thickness and so ridge spreading rate. We argue that the horizontal stress at oceanic spreading centers is close to the normal faulting stress, thus the most feasible explanation for this discrepancy is that the magma supply from the magma chamber is limited so that the magma pressure drops as the dike propagates. We show that a meter-wide dike could be produced if the magma pressure is lower than the maximum, a few hundred meters below the seafloor as measured by magma head. For cases with thick axial lithosphere and/or very limited magma supply a single dike can only partially release stress accumulated during amagmatic stretching periods, thus an episode of dikes is needed to fully release them.

Acknowledgements

We thank M. Helen-Cormier, P. Kelemen, and A. Gudmundsson for their helpful discussions and suggestions. C. P. Jaupart and G. A. Valentine's review has greatly improved the paper. J. Karson kindly provided us dike width data from Hess Deep.

References

Baran, J.M., et al., 2005. Variations in upper crustal structure due to variable mantle temperature along the Southeast Indian Ridge. Geochem. Geophys. Geosyst. 6, 21.

Barclay, A.H., et al., 1998. Seismic structure and crustal magmatism at the Mid-Atlantic Ridge, 35 degrees N. J. Geophys. Res.-Sol. Ea 103, 17827–17844.

Birch, F., 1966. Compressibility: elastic constants. Handbook of Physical Constants, pp. 567–590.

Brandsdottir, B., et al., 1997. Faroe–Iceland Ridge experiment. 2. Crustal structure of the Krafla central volcano. J. Geophys. Res.-Sol. Ea 102, 7867–7886.

Bruce, P.M., Huppert, H.E., 1989. Thermal control of basaltic fissure eruptions. Nature 342, 665–667.

Buck, W.R., 2006. On the frequency of dike intrusion episodes at spreading centers. Eos Trans. AGU 87 (52) Fall Meet. Suppl., Abstract T41B-1566.

Buck, W.R., et al., 2006. Tectonic stress and magma chamber size as controls on dike propagation: constraints from the 1975–1984

Krafla rifting episode. J. Geophys. Res.-Sol. Ea 111, doi:10.1029/2005JB003879.

Crawford, W.C., Webb, S.C., 2002. Variations in the distribution of magma in the lower crust and at the Moho beneath the East Pacific Rise at 9 degrees–10 degrees N. Earth Planet. Sci. Lett. 203, 117–130.

Crouch, S.L., Starfield, A.M., 1983. Boundary Element Methods in Solid Mechanics. George Allen & Unwin, London.

Delaney, J.R., et al., 1998. The quantum event of oceanic crustal accretion: impacts of diking at mid-ocean ridges. Science 281, 222–230.

Einarsson, P., Brandsdottir, B., 1980. Seismological evidence for lateral magma intrusion during the July 1978 deflation of the Krafla Volcano in NE Iceland. J. Geophys.-Z. Geophys. 47, 160–165.

Fialko, Y.A., Rubin, A.M., 1998. Thermodynamics of lateral dike propagation: implications for crustal accretion at slow spreading mid-ocean ridges. J. Geophys. Res.-Sol. Ea 103, 2501–2514.

Foulger, G.R., et al., 2003. Icelandic-type crust. Geophys. J. Int. 155, 567–590.

Gudmundsson, A., 1983. Form and dimensions of dykes in Eastern Iceland. Tectonophysics 95, 295–307.

Gudmundsson, A., 1995. The geometry and growth of dykes. In: Baer, G., Heimann, A., Rotterdam, V.T. (Eds.), Physics and Chemistry of Dykes.

Harper, G.D., 1984. The Josephine Ophiolite, Northwestern California. Geol. Soc. Am. Bull. 95, 1009–1026.

Karson, J.A., 1999. Geological investigation of a lineated massif at the Kane Transform Fault: implications for oceanic core complexes. Philos. Trans. Royal Soc. A 357, 713–736.

Karson, J.A., et al., 2002. Internal structure of uppermost oceanic crust along the Western Blanco Transform Scarp: implications for subaxial accretion and deformation at the Juan de Fuca Ridge. J. Geophys. Res.-Sol. Ea 107, 24.

Kelemen, P.B., Aharonov, E., 1998. Periodic formation of magma fractures and generation of layered gabbros in the lower crust beneath oceanic spreading ridges. In: Buck, W.R. (Ed.), Faulting and Magmatism at Mid-Ocean Ridges, p. 106. AGU Monograph.

Kidd, R.G.W., 1977. Model for process of formation of upper oceanic crust. Geophys. J. R. Astron. Soc. 50, 149–183.

Lin, J., Parmentier, E.M., 1989. Mechanisms of lithospheric extension at mid-ocean ridges. Geophys. J. Int. 96, 1–22.

Lister, J.R., 1995. Fluid-mechanical models of the interaction between solidification and flow in dykes. In: Baer, G., Heimann, A., Rotterdam, VT (Eds.), Physics and Chemistry of Dykes.

Macdonald, G.A., et al., 1986. Volcanoes in the Sea: the Geology of Hawaii, Honolulu, 2nd ed. University of Hawaii press, Hawaii.

Macdonald, K.C., et al., 1996. Volcanic growth faults and the origin of Pacific abyssal hills. Nature 380, 125–129.

Magde, L.S., Sparks, D.W., 1997. Three-dimensional mantle upwelling, melt generation, and melt migration beneath segment slow spreading ridges. J. Geophys. Res.-Sol. Ea 102, 20571–20583.

Mogi, K., 1958. Relations of eruptions of various volcanoes and the deformation of the ground surfaces around them. Bull. Earthq. Res. Inst. Univ. Tokyo 39, 99–134.

Oliver, G.J.H., McAlpine, R.R., 1998. Occurrence of a sheeted dolerite dyke complex in the Ballantrae Ophiolite, Scotland. Geol. Mag. 135, 509–517.

Pollard, D.D., et al., 1983. Surface deformation in volcanic rift zones. Tectonophysics 94, 541–584.

Purdy, G.M., et al., 1992. Relationship between spreading rate and the seismic structure of midocean ridges. Nature 355, 815–817.

Qin, R., et al., 2007. Comment on "Mechanics of Tidally Driven Fractures in Europa's Ice Shell" by S. Lee, R.T. Pappalardo, and N.C. Makris [2005. Icarus 177, 367–379]. Icarus 189, 595–597.

Reinecker, J., et al., 2004. The 2004 release of the World Stress Map. available online at www.world-stress-map.org.

Rosencrantz, E., 1983. The structure of sheeted dikes and associated rocks in North Arm Massif, Bay of Islands ophiolite complex, and the intrusive process at oceanic spreading centers. Can. J. Earth Sci. 20, 787–801.

Rubin, A.M., 1990. A comparison of rift-zone tectonics in Iceland and Hawaii. B. Volcanol. 52, 302–319.

Rubin, A.M., Pollard, D.D., 1988. Dike-induced faulting in rift zones of Iceland and Afar. Geology 16, 413–417.

Sinton, J., et al., 2002. Volcanic eruptions on mid-ocean ridges: new evidence from the superfast spreading East Pacific Rise, 17 degrees–19 degrees S. J. Geophys. Res.-Sol. Ea 107, 21.

Sinton, J.M., Detrick, R.S., 1992. Midocean ridge magma chambers. J. Geophys. Res.-Sol. Ea 97, 197–216.

Sohn, R.A., et al., 1998. Seismic and hydrothermal evidence for a cracking event on the East Pacific Rise crest at 9 degrees 50′ N. Nature 396, 159–161.

Tolstoy, M., et al., 2006. A sea-floor spreading event captured by seismometers. Science 314, 1920–1922.

Tryggvason, E., 1994. Surface deformation at the Krafla Volcano, North Iceland, 1982–1992. B. Volcanol. 56, 98–107.

Turcotte, D.L., Schubert, G., 2002. Geodynamics. Cambridge University Press, New York.

Umino, S., et al., 2003. Along-strike variation of the sheeted dike complex in the Oman Ophiolite: insights into subaxial ridge segment structures and the magma plumbing system. Geochem. Geophys. Geosyst. 4, 34.

Valentine, G.A., Krogh, K.E.C., 2006. Emplacement of shallow dikes and sills beneath a small basaltic volcanic center — the role of pre-existing structure (Paiute Ridge, southern Nevada, USA). Earth Planet. Sci. Lett. 246, 217–230.

Valentine, G.A., Perry, F.V., 2007. Tectonically controlled, time-predictable basaltic volcanism from a lithospheric mantle source (central Basin and Range Province, USA). Earth Planet. Sci. Lett. 261, 201–216.

Weertman, J., 1973. Can a water-filled crevasse reach the bottom surface of a glacier? Symposium on the Hydrology of Glaciers, Cambridge 7–13 Sept. 1969. International Association of Hydrologic Sciences, Cambridge, pp. 139–145.

Wright, D.J., et al., 1995. Crustal fissuring and its relationship to magmatic and hydrothermal processes on the East Pacific Rise Crest (9 degrees-12′ to 54′N). J. Geophys. Res.-Sol. Ea 100, 6097–6120.

Wright, T.J., et al., 2006. Magma-maintained rift segmentation at continental rupture in the 2005 Afar dyking episode. Nature 442, 291–294.